DNA Damage and Cellular Stress Responses

Molecular Cancer Research

Inhibition of Eg5 Acts Synergistically with Checkpoint Abrogation in Promoting Mitotic Catastrophe

Yue Chen, Jeremy P.H. Chow, and Randy Y.C. Poon

Abstract

The G_2 DNA damage checkpoint is activated by genotoxic agents and is particularly important for cancer therapies. Overriding the checkpoint can trigger precocious entry into mitosis, causing cells to undergo mitotic catastrophe. But some checkpoint-abrogated cells can remain viable and progress into G_1 phase, which may contribute to further genome instability. Our previous studies reveal that the effectiveness of the spindle assembly checkpoint and the duration of mitosis are pivotal determinants of mitotic catastrophe after checkpoint abrogation. In this study, we tested the hypothesis whether mitotic catastrophe could be enhanced by combining genotoxic stress, checkpoint abrogation, and the inhibition of the mitotic kinesin protein Eg5. We found that mitotic catastrophe induced by ionizing radiation and a CHK1 inhibitor (UCN-01) was exacerbated after Eg5 was inhibited with either siRNAs or monastrol. The combination of DNA damage, UCN-01, and monastrol sensitized cancer cells that were normally resistant to checkpoint abrogation. Importantly, a relatively low concentration of monastrol, alone not sufficient in causing mitotic arrest, was already effective in promoting mitotic catastrophe. These experiments suggest that it is possible to use sublethal concentrations of Eg5 inhibitors in combination with G_2 DNA damage checkpoint abrogation as an effective therapeutic approach. *Mol Cancer Res; 10(5); 626–35. ©2012 AACR.*

Introduction

DNA checkpoints are essential mechanisms that halt cell-cycle progression after DNA damage. Genetic defects of checkpoint components or agents that abrogate the checkpoints can promote genome instability and cell death. The G_2 DNA damage checkpoint, which is particularly important for radiotherapies, prevents damaged cells from entering into mitosis. CDK1 (cyclin-dependent kinase 1) is one of the major protein kinases for promoting mitosis (1). The checkpoint involves the activation of ATM (ataxia telangiectasia mutated) and ATR (ATM- and Rad3-related) kinases, which then activate CHK1 and CHK2. These in turn alter the balance of control between CDC25 and WEE1, thereby increasing the inhibitory phosphorylation of CDK1 (2).

Uncoupling of the G_2 DNA damage checkpoint can promote unscheduled activation of CDK1, thereby triggering premature mitosis. The checkpoint-abrogated cells then undergo a process termed mitotic catastrophe (3). The cells often undergo apoptosis directly during the aberrant mitosis. Alternatively, checkpoint-abrogated cells can exit mitosis and progress into the next interphase. Importantly, cells that exit mitosis and survive can contribute to further genome instability, yielding more aggressive tumors that are more resistant to subsequent therapies. Hence, a salient factor for therapies based on the approach of checkpoint abrogation is how to eliminate cancer cells during the first mitosis.

Previously, we have used long-term time-lapse microscopy to track the fates of individual cells after the ionizing radiation (IR)-mediated G_2 DNA damage checkpoint is abrogated with the CHK1 inhibitor UCN-01 (4). We found that the extent of mitotic cell death is closely related to the duration of mitosis. In support of this, mitotic cell death was suppressed by weakening of the spindle assembly checkpoint, either through depletion of MAD2 or overexpression of the MAD2-binding protein $p31^{comet}$. Conversely, delaying of mitotic exit by depletion of either $p31^{comet}$ or CDC20 tipped the balance toward mitotic cell death. Significantly, these results indicate that extending mitosis by activating the spindle assembly checkpoint has the same effect on mitotic cell death as using a higher dose of IR. An implication is that lower concentrations of DNA-damaging agents can be used (thus causing less general toxicity) if UCN-01 is administered together with a drug that can procrastinate mitotic exit.

On the basis of these premises, we investigated whether drugs that extend mitosis can be used in conjunction with IR and UCN-01 to promote more mitotic cell death. Eg5 [kinesin spindle protein (KSP), HKSP, KNSL1, TRIP5, or kinesin family member 11 (KIF11)] is a plus-end directed

Authors' Affiliation: Division of Life Science and Center for Cancer Research, Hong Kong University of Science and Technology, Clear Water Bay, Kowloon, Hong Kong

Note: Supplementary data for this article are available at Molecular Cancer Research Online (http://mcr.aacrjournals.org/).

Corresponding Author: Randy Y.C. Poon, Division of Life Science, Hong Kong University of Science and Technology, Clear Water Bay, Kowloon, Hong Kong. Phone: 852-23588703; Fax: 852-23581552; E-mail: rycpoon@ust.hk

doi: 10.1158/1541-7786.MCR-11-0491

microtubule motor of the kinesin-5 family (5) which localizes along the interpolar spindle microtubules and spindle poles (6). Eg5 is implicated in various mitotic microtubule functions including microtubule cross-linking, antiparallel microtubule sliding, and bipolar spindle formation, ensuring the fidelity of chromosome segregation.

The expression of Eg5 is closely related to cell proliferation and cancer. For example, overexpression of Eg5 is found in bladder cancer (7) and pancreatic cancer (8). Furthermore, transgenic mice overexpressing Eg5 are prone to develop a variety of tumors (9). These and other observations favor Eg5 as an attractive target for chemotherapy. Using a phenotypic screen that was designed to identify antimitotic compounds that do not directly interfere with microtubule dynamics, monastrol was identified as the first small-molecule inhibitor of Eg5 (10). Monastrol induces the formation of monoastral spindle, resulting in an activation of the spindle assembly checkpoint followed by apoptosis (11). Nevertheless, the clinical potential of monastrol is limited because of its relatively weak Eg5 inhibitory activity and the variety of side effects associated with high dosages.

Here, we showed that mitotic catastrophe induced by IR and UCN-01 was enhanced after Eg5 was inhibited with either siRNAs or monastrol. Importantly, a relatively low concentration of monastrol, alone not sufficient to cause mitotic arrest, was already effective in promoting mitotic catastrophe after checkpoint abrogation. These proof of principle experiments underscore the possibility of using sublethal doses of existing drugs including monastrol, IR, and UCN-01 as effective combinatorial therapeutic approaches.

Materials and Methods

Materials

All reagents were obtained from Sigma-Aldrich unless stated otherwise.

Cell culture and cell growth analysis

HeLa (cervical carcinoma), H1299 (non–small cell lung carcinoma), and HCT116 (colorectal carcinoma) were obtained from American Type Culture Collection. U2OS (osteosarcoma) Tet-On cell line was obtained from Clontech. No authentication was done by the authors. The HeLa cell line used in this study was a clone that expressed the Tet repressor (12). HeLa cells expressing histone H2B-GFP were generated as described previously (13). Cells were propagated in Dulbecco's Modified Eagle's Medium supplemented with 10% (v/v) calf serum (for HeLa) or fetal bovine serum (for other cells; Invitrogen) and 50 U/mL penicillin-streptomycin (Invitrogen) in a humidified incubator at 37°C in 5% CO_2. Unless stated otherwise, cells were treated with the following reagents at the indicated final concentration: monastrol (Enzo Life Sciences;100 μmol/L) and UCN-01 (100 nmol/L). Trypan blue analyses were conducted as described (14). For clonogenic survival assays, 10,000 cells were irradiated with indicated doses of IR and seeded onto 60-mm dishes. After 16 hours, the cells were either mock-treated or exposed to the indicated concentrations of UCN-01 and/or monastrol for another 16 hours. Both floating and attached cells were collected by centrifugation. The cells (100) were seeded onto 12-well plates. Fresh medium were replenished every 3 days. After 2 weeks, colonies were fixed with methanol/acetic acid (2:1 v/v) and visualized by staining with 2% (w/v) crystal violet in 20% methanol.

RNA interference

Stealth siRNAs targeting Eg5 (CCGAAGUGUUGUUUGUCCAAUUCUA and GAGAGAUUCUGUGCUUUGGAGGAAA), CHK1 (GGCUUGGCAACAGUAUUUCGGUAUA), and control siRNA were obtained from Invitrogen. Cells were transfected with siRNA using Lipofectamine RNAiMAX (Invitrogen) according to the manufacturer's instructions.

Ionizing radiation

IR was delivered with a caesium^{137} source from a MDS Nordion Gammacell 1000 Elite Irradiator. Unless stated otherwise, cells were irradiated with a dose of 15 Gy.

Live cell imaging

Cells were seeded onto poly-lysine–coated glass plates and imaged with a TE2000E-PFS inverted fluorescent microscope (Nikon) equipped with a SPOT BOOST EMCCD camera (Diagnostic Instrument) and a INU-NI-F1 temperature, humidity, and CO_2 control system (Tokai Hit). Data acquisition were carried out at 3 min/frame.

Flow cytometry

Flow cytometric analysis after propidium iodide staining was conducted as described previously (14).

Antibodies and immunologic methods

Monoclonal antibodies against β-actin (15), cyclin A2 (16), and cyclin B1 (13) were obtained from sources as described previously. Polyclonal antibodies against phospho-CDK1^{Tyr15} (Cell Signaling Technology), phospho-histone H3^{Ser10} (Santa Cruz Biotechnology), PLK1 (Santa Cruz Biotechnology) and monoclonal antibodies against cleaved PARP (Asp214; BD Biosciences) and Eg5 (BD Biosciences) were obtained from the indicated suppliers. Immunoblotting and immunoprecipitation were carried out as described (17).

Results

Expression of Eg5 during checkpoint abrogation

Before investigating the contribution of Eg5 on mitotic catastrophe, we first examined the expression of Eg5 after checkpoint abrogation. IR mainly activated the G_2 DNA damage checkpoint in HeLa cells (in part due to the fact that p53 is inactivated by human papilloma virus E6), which could be effectively overridden with the CHK1 inhibitor UCN-01 (4). Figure 1A shows that Eg5 accumulated during the IR-induced G_2 phase arrest. In accordance with the activation of the checkpoint, proteins that typically accumulate in G_2 phase such as PLK1 as well as Tyr15-phosphorylated CDK1 also increased after irradiation. As

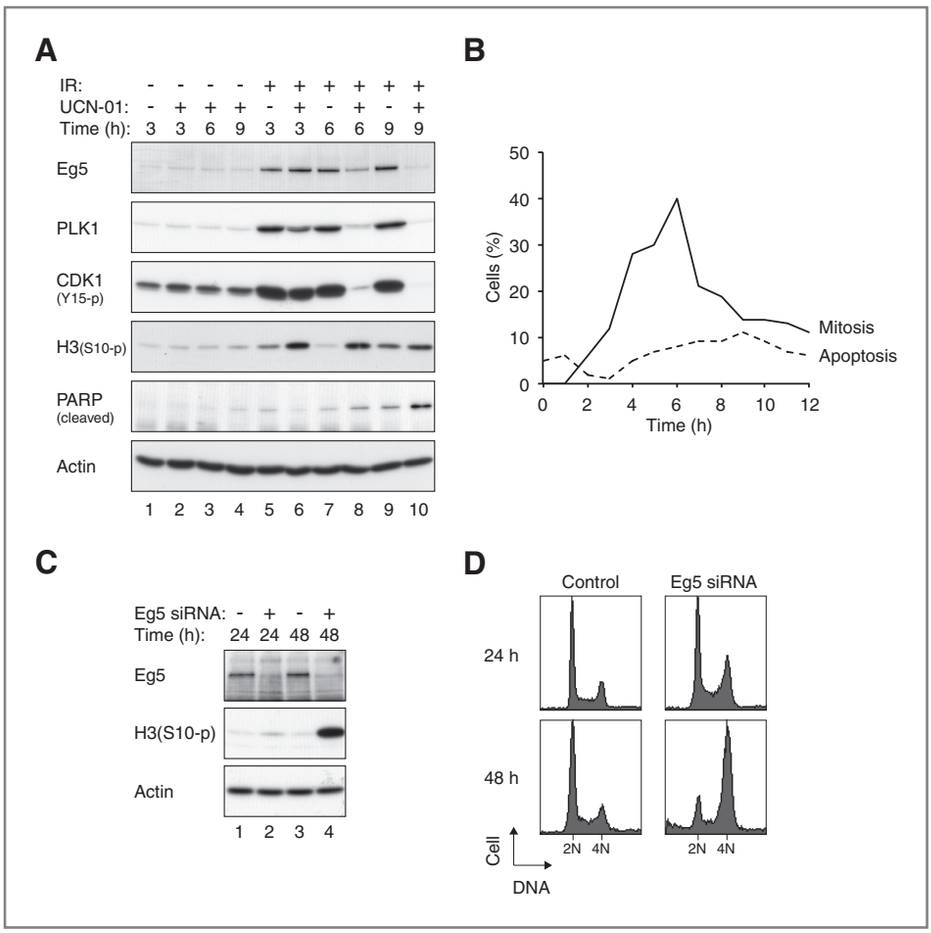

Figure 1. Eg5 is expressed during checkpoint abrogation and can be downregulated with siRNA. A, expression of Eg5 during checkpoint abrogation. HeLa cells were either mock treated or irradiated as indicated. After incubation for 16 hours, the cells were treated with either buffer or UCN-01. At the indicated time points after UCN-01 addition, the cells were harvested and analyzed with immunoblotting. Equal loading of lysates was confirmed by immunoblotting for actin. B, precocious mitosis after checkpoint abrogation. HeLa cells expressing histone H2B-GFP were irradiated, cultured for 16 hours, followed by UCN-01 treatment. The cells were then subjected to time-lapse microscopy to track individual cells for 12 hours ($n = 50$). The percentage of cells undergoing mitosis (solid line) and apoptosis (dotted line) was quantified. C, depletion of Eg5 promotes histone $H3^{Ser10}$ phosphorylation. HeLa cells were transfected with either control or Eg5 siRNA and harvested at the indicated time points. Lysates were prepared and analyzed with immunoblotting. Actin analysis was included to assess protein loading and transfer. D, depletion of Eg5 induces an accumulation of G_2–M cells. Cells were transfected with either control or Eg5 siRNA and harvested at the indicated time points. The cells were fixed, stained with propidium iodide, and analyzed with flow cytometry. The positions of 2N and 4N DNA contents are indicated.

expected, abrogation of the checkpoint with UCN-01 lead to premature mitosis, as revealed by an increase in histone $H3^{Ser10}$ phosphorylation (lane 6). UCN-01–treated cells were only in mitosis transiently before they entered the next G_1 phase (4). This correlated with the decrease in PLK1 and phospho-$CDK1^{Tyr15}$ at later time points (lanes 8 and 10). Likewise, Eg5 expression also decreased as the cells exited mitosis. The persistent of histone $H3^{Ser10}$ phosphorylation at later time points was probably due to a portion of cells undergoing apoptosis. This is also corroborated by the increase in the cleavage of the caspase substrate PARP. In agreement with this, live cell imaging revealed that UCN-01 induced a transient increase in mitosis in IR-treated cells (Fig. 1B). These data verified the presence of Eg5 during checkpoint abrogation.

Downregulation of Eg5 promotes mitotic catastrophe in checkpoint-abrogated cells

The identity of the Eg5 band as detected by immunoblotting was further verified by siRNA-mediated downregulation (Fig. 1C). Histone $H3^{Ser10}$ was highly phosphorylated after siRNA transfection (in particular at 48 hours), indicating that cells were enriched in mitosis in the absence of Eg5. This mitotic delay was also verified by the accumulation of cells with G_2–M DNA contents (Fig. 1D) and the rounding up of cells under microscopy (data not shown).

We next studied the effects of Eg5 depletion on UCN-01–induced checkpoint abrogation. Cells were transfected with Eg5 siRNA before irradiation. After 16 hours, the G_2-arrested cells were treated with UCN-01. Figure 2A

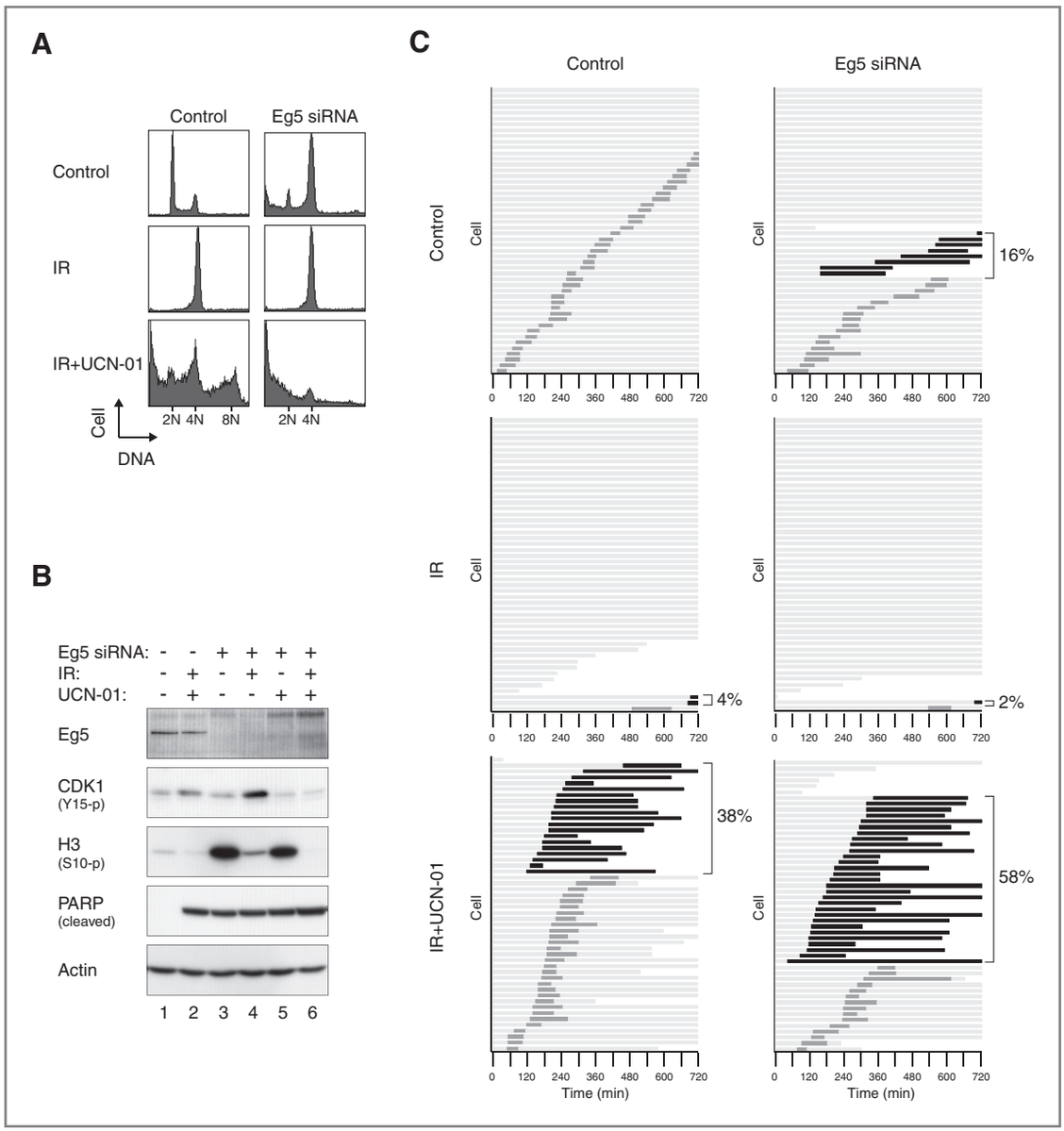

Figure 2. Depletion of Eg5 enhances UCN-01–mediated mitotic catastrophe. A, depletion of Eg5 increases sub-G_1 cells after checkpoint abrogation. HeLa cells were transfected with either control or Eg5 siRNA. After 6 hours, the cells were irradiated, cultured for 16 hours, and treated with UCN-01. After 12 hours, DNA contents were analyzed with flow cytometry. B, verification of Eg5 depletion by immunoblotting. Cells were transfected and treated as in (A). Cell-free extracts were prepared and subjected to immunoblotting analysis for the indicated proteins. Uniform loading of lysates was verified by immunoblotting for actin. C, time-lapse microscopy. HeLa cells expressing histone H2B-GFP were transfected with either control or Eg5 siRNA. After 6 hours, the cells were untreated, irradiated and cultured for 16 hours, or irradiated (16 hours) followed by UCN-01 treatment. The cells were then subjected to time-lapse microscopy to track individual cells for 12 hours ($n = 50$). Key: light gray, interphase; dark gray, mitosis (from DNA condensation to anaphase); black, mitotic catastrophe (from DNA condensation to cell death); truncated bars, cell death. Mitotic catastrophe was defined as cells that directly undergo apoptosis during the unscheduled mitosis. The time of cell death after mitosis is defined by the death of one of the daughters. The percentages of cells that underwent mitotic catastrophe are shown (a portion of cells that were still trapped in mitosis at the end of the 12-hour imaging was also categorized as mitotic catastrophe).

shows that IR induced a G_2 arrest as anticipated. Irradiated Eg5-depleted cells were also arrested in G_2 (instead of mitosis) because of the low level of histone $H3^{Ser10}$ phosphorylation (Fig. 2B, lane 4). In agreement with previous results (4), UCN-01 triggered checkpoint bypass, resulting in a subset of cells undergoing mitotic catastrophe or abnormal mitosis (typically with cytokinesis failure), giving rise to the sub-G_1 and >4N populations, respectively (Fig. 2A). In this study, mitotic catastrophe was defined as cells that directly undergo apoptosis during the unscheduled mitosis. Importantly, significantly more cells underwent cell death–associated mitotic catastrophe

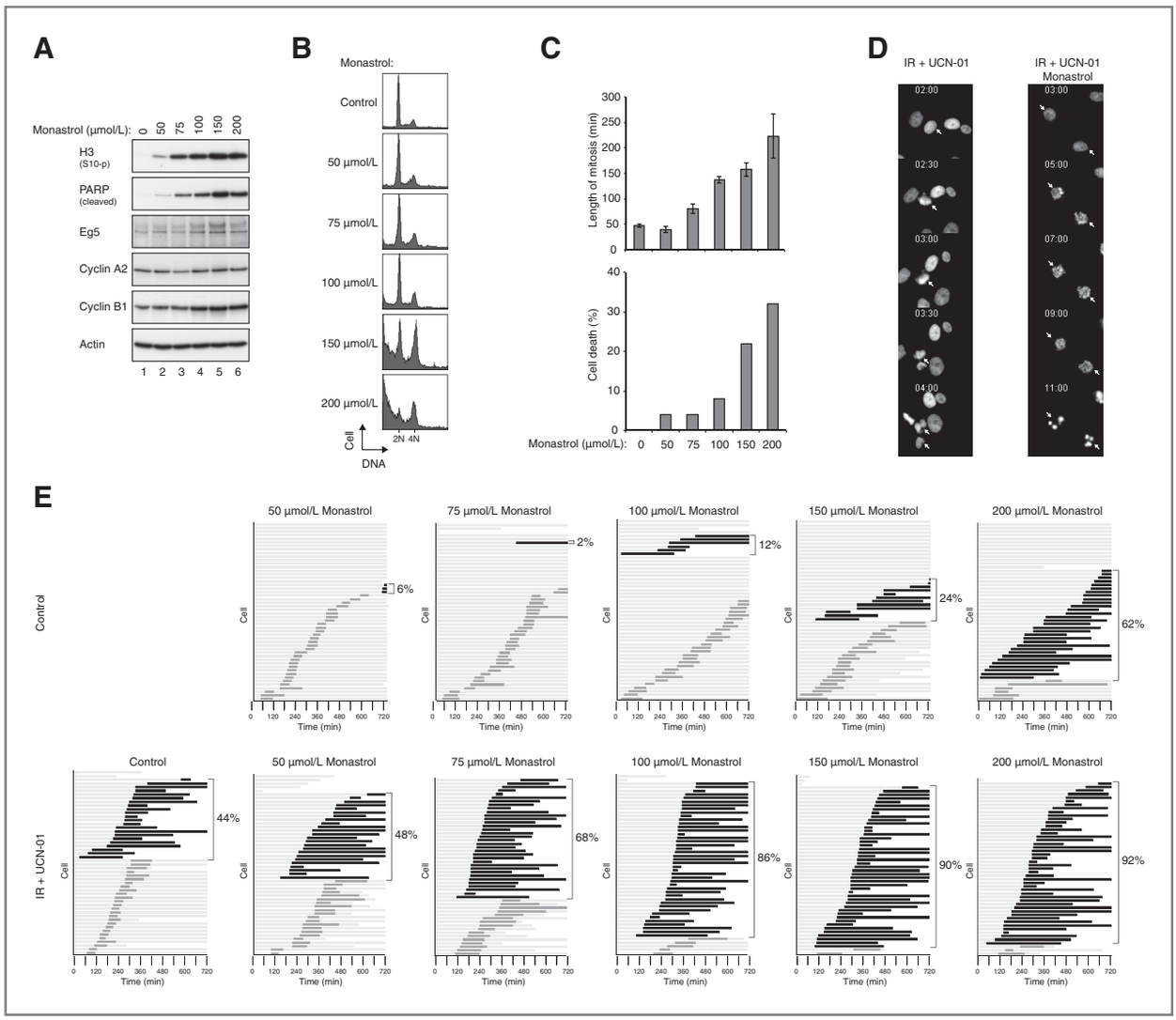

Figure 3. Monastrol promotes the mitotic catastrophe triggered by IR and UCN-01. A, mitotic arrest and cell death are triggered by monastrol in a concentration-dependent manner. HeLa cells were treated with the indicated concentrations of monastrol. After incubation for 24 hours, lysates were prepared and the expression of the indicated proteins was detected by immunoblotting. Equal loading of lysates was confirmed by immunoblotting for actin. B, concentration-dependent accumulation of G_2–M and sub-G_1 populations by monastrol. Cells were treated exactly as in (A). After incubation for 24 hours, the cells were fixed, stained with propidium iodide, and analyzed with flow cytometry. The positions of 2N and 4N DNA contents are indicated. C, mitotic catastrophe is induced by high concentrations of monastrol. HeLa cells expressing histone H2B-GFP were treated with different concentrations of monastrol. The cells were then subjected to time-lapse microscopy to track individual cells for 12 hours ($n = 50$). The duration of mitosis (from DNA condensation to anaphase; only counting the cells that successfully finished mitosis) was quantified (average ±90% confidence coefficient; top). The percentage of cells undergoing cell death during the imaging period was also quantified (bottom). D, monastrol promotes mitosis containing monoastral spindles after IR and UCN-01 treatments. HeLa cells expressing histone H2B-GFP were irradiated. After 16 hours, the cells were treated with UCN-01 either in the absence or presence of 100 μmol/L of monastrol. The cells were then tracked with time-lapse microscopy to detect the histone H2B-GFP. Representative mitotic cells are shown (arrows). The complete videos are shown in Supplementary Video S1 and S2. E, monastrol promotes mitotic catastrophe triggered by IR and UCN-01. HeLa cells expressing histone H2B-GFP were either untreated or irradiated (16 hours) followed by treatments with UCN-01. The cells were incubated with different concentrations of monastrol. The cells were then subjected to time-lapse microscopy to track individual cells for 12 hours ($n = 50$). Key: light gray, interphase; dark gray, mitosis (from DNA condensation to anaphase); black, mitotic catastrophe (from DNA condensation to cell death); truncated bars, cell death. The percentages of cells that underwent mitotic catastrophe are shown (a portion of cells that were still trapped in mitosis at the end of the 12-hour imaging was also categorized as mitotic catastrophe). Quantification of the data can be found in (C).

after Eg5 was downregulated. The same results were obtained using another siRNA targeting a different region of Eg5, indicating that the specificity of the effects (data not shown).

Because of the various cell fates after checkpoint abrogation, the extent of cell death could not be accurately revealed when the entire cell population was analyzed. For example, although the increase in sub-G_1 population was

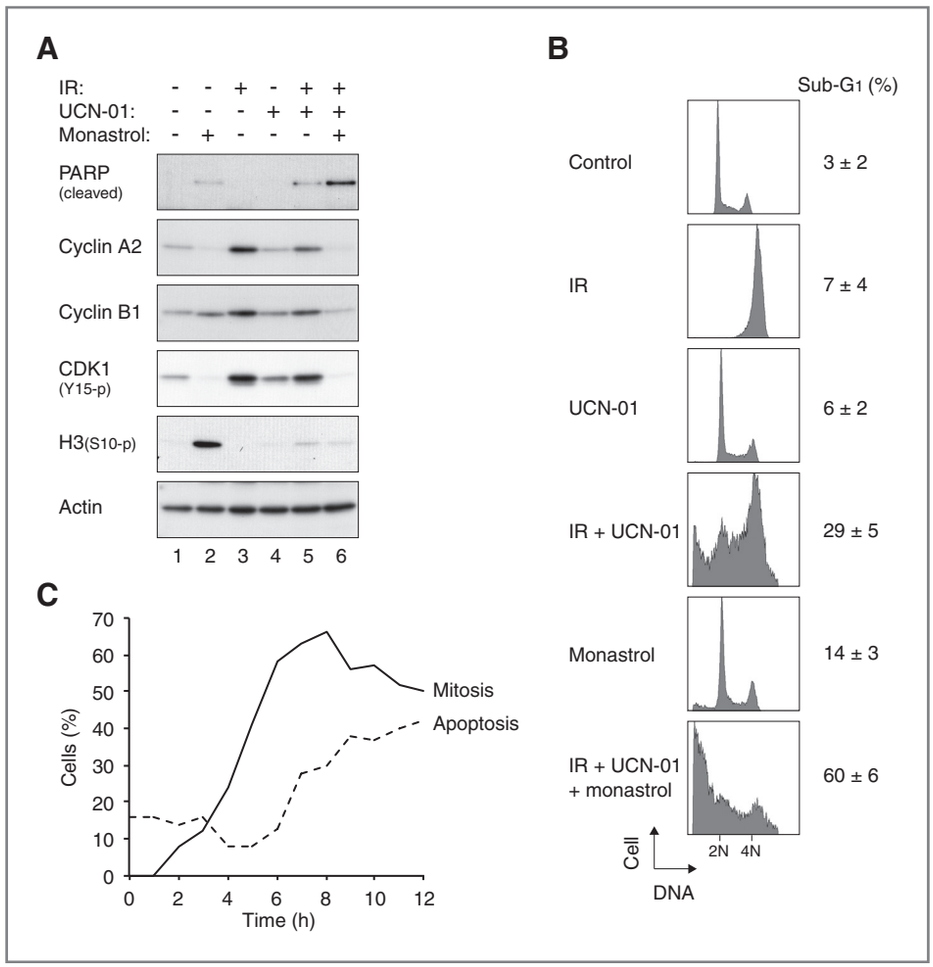

Figure 4. Mitotic catastrophe triggered by IR and UCN-01 can be enhanced by a low concentration of monastrol. A, monastrol increases PARP cleavage after checkpoint abrogation. HeLa cells were either mock-treated or irradiated and incubated for 16 hours. The cells were then treated with a combination of UCN-01 and 100 μmol/L of monastrol as indicated. After 24 hours, lysates were prepared and analyzed with immunoblotting. Equal loading of lysates was confirmed by immunoblotting for actin. B, monastrol increases sub-G_1 population after checkpoint abrogation. Cells were treated exactly as in (A). After 24 hours, the cells were fixed, stained with propidium iodide, and analyzed with flow cytometry. The positions of 2N and 4N DNA contents as well as the percentage of sub-G_1 population (mean ± SD of 3 independent experiments) are indicated. C, monastrol induces mitotic block and massive cell death in checkpoint-abrogated cells. HeLa cells expressing histone H2B-GFP were irradiated, cultured for 16 hours, followed by treatment with UCN-01 and monastrol. The cells were then subjected to time-lapse microscopy to track individual cells for 12 hours ($n = 50$). The percentage of cells undergoing mitosis (solid line) and apoptosis (dotted line) was quantified.

conspicuous in the absence of Eg5 (Fig. 2A), the increase in cleaved PARP signal was only marginal (Fig. 2B). To obtain more quantitative data on different cell fates, time-lapse microscopy was used to track individual cells after checkpoint abrogation. HeLa cells expressing histone H2B-GFP were used, allowing us to simultaneous image both cell morphology and DNA. Figure 2C shows that most control cells entered mitosis once over the 12-hour imaging period. In contrast, mitosis was attenuated after irradiation. This cell-cycle arrest was overcome after the addition of UCN-01, with approximately 80% of the cells entering mitosis within 4 hours. As expected, a subset of the checkpoint-abrogated cells underwent cell death during mitosis. Knockdown of Eg5 caused a slight increase in mitotic catastrophe in unperturbed cell cycle. Furthermore, neither the IR-mediated cell-cycle arrest nor the extent of UCN-01–mediated checkpoint bypass was affected in Eg5-depleted cells. Nevertheless, markedly more Eg5-depleted cells underwent mitotic catastrophe after checkpoint abrogation than control cells. Taken together, these observations revealed that down-regulation of Eg5 sensitizes cells to mitotic catastrophe caused by IR and UCN-01.

Mitotic catastrophe after checkpoint bypass is enhanced by monastrol

The above results suggest that Eg5 inactivation may enhance checkpoint abrogation–based cancer therapies. To test this idea, we evaluated the effects of monastrol, a well-characterized small inhibitor of Eg5, with IR and UCN-01. As expected, monastrol induced mitotic arrest (histone $H3^{Ser10}$ phosphorylation) and cell death (cleaved PARP) in a concentration-dependent manner (Fig. 3A). In accordance with these, treatment with monastrol promoted the accumulation of cells containing G_2–M and sub-G_1 DNA contents (Fig. 3B). Using time-lapse microscopy to track the fate of individual cells, we found that monastrol stimulated a concentration-dependent increase in mitotic duration (Fig. 3E, quantified in Fig. 3C). Moreover, increasing dosage of monastrol progressively increased the portion of cells undergoing mitotic cell death (Fig. 3E, quantified in Fig. 3C). These cells generally underwent a prolonged mitosis with condensed chromosomes in a rosette-like configuration, typical of cells containing monoastral spindle, before undergoing cell death.

We next combined different concentrations of monastrol with IR and UCN-01 treatments and monitored the cells with time-lapse microscopy (Fig. 3E). Challenging cells with 100 μmol/L of monastrol alone did not induce substantial cell death. This was evident even when the cells were followed for more than a period of 24 hours (Supplementary Fig. S1). Compared with cells treated with IR and UCN-01 only, addition of 100 μmol/L of monastrol substantially increased the percentage of cells undergoing mitotic catastrophe (from ~40%–90%). Although higher concentrations of monastrol also induced similar increase in mitotic catastrophe, they already triggered significant level of mitotic catastrophe even in the absence of IR and UCN-01 (Fig. 3E). As expected, while IR- and UCN-01–treated cells could undergo a relatively normal mitosis, no metaphase plate was formed in the presence of monastrol (Fig. 3D).

The above results were further confirmed by immunoblotting and flow cytometry. The level of cleaved PARP in cells treated with IR, UCN-01, and 100 μmol/L of monastrol was higher than in cells receiving the individual treatments separately (Fig. 4A). Likewise, the sub-G_1 population was significantly higher in the presence of monastrol than in cells challenged with IR and UCN-01 only (Fig. 4B). These data are consistent with the time-dependent accumulation of mitotic cells and massive apoptotic cell death after the irradiated cells were treated with UCN-01 and monastrol (Fig. 4C; compared with cells treated with IR and UCN-01 only in Fig. 1B).

To ensure that the effects of UCN-01 was specific to inhibition of CHK1, we also depleted CHK1 using siRNA. Similar to after UCN-01 treatment, depletion of CHK1 abolished the IR-mediated cell-cycle arrest (Supplementary Fig. S2). Mitotic catastrophe was significantly increased in the presence of monastrol.

To verify that the mitotic catastrophe caused by monastrol was not limited to HeLa cells, we next carried out the same treatments on another cell line. The presence of Eg5 protein in H1299, HCT116, and U2OS was confirmed by immunoblotting (Fig. 5A). H1299 cells were selected because they expressed high level of Eg5. Furthermore, unlike HeLa cells, H1299 cells were relatively resistant to the mitotic catastrophe mediated by IR and UCN-01. Live cell imaging revealed that 80% of cells survived mitosis induced after IR and UCN-01 treatments (4). Consistent with this, IR

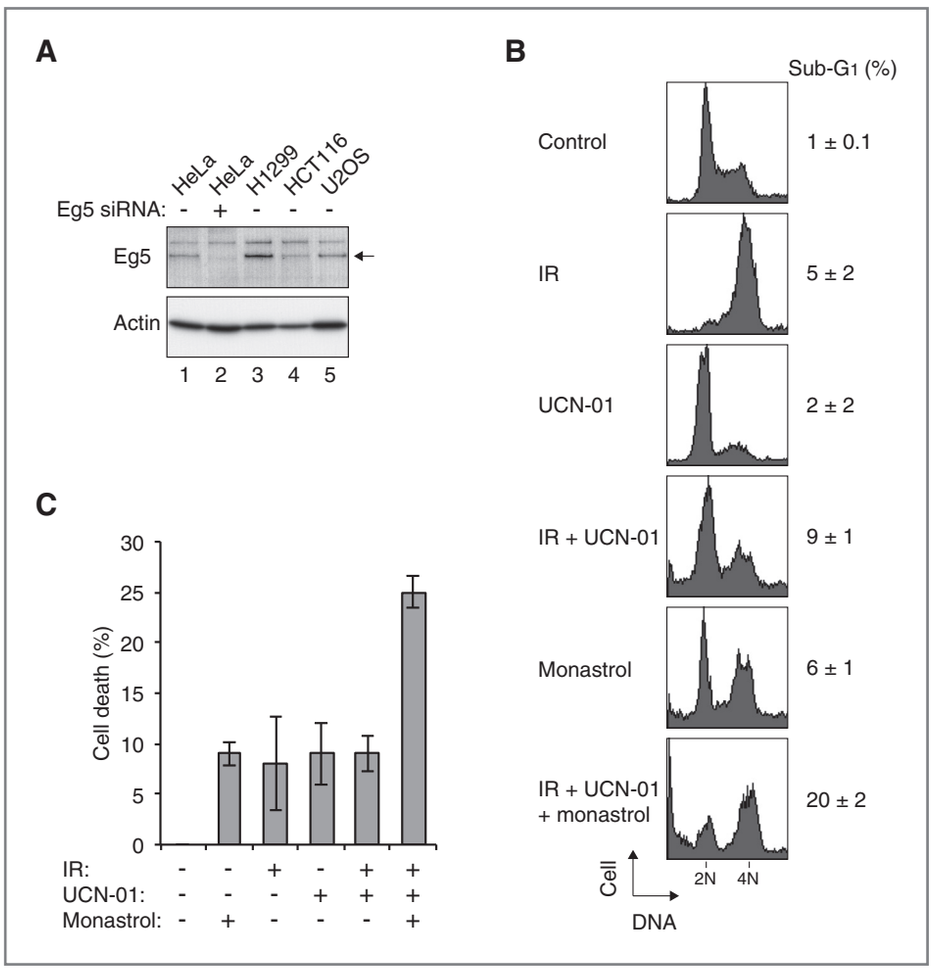

Figure 5. Monastrol enhances mitotic catastrophe in H1299 cells. A, expression of Eg5 in different cell lines. Lysates from asynchronously growing H1299, HCT116, and U2OS were subjected to immunoblotting for Eg5. HeLa cells transfected with control or Eg5 siRNA served as controls. Actin analysis was included to assess protein loading and transfer. B, monastrol increases sub-G_1 population after checkpoint abrogation. H1299 cells were either mock-treated or irradiated and incubated for 16 hours. The cells were treated with a combination of UCN-01 and 100 μmol/L of monastrol as indicated. After 48 hours, the cells were fixed, stained with propidium iodide, and analyzed with flow cytometry. The positions of 2N and 4N DNA contents as well as the percentage of sub-G_1 population (mean ± SD of 3 independent experiments) are indicated. C, monastrol increases cell death after checkpoint abrogation. H1299 cells were treated exactly as in (B). Viability was determined with Trypan blue exclusion assay. Mean ± SD of 3 independent experiments are shown.

followed by UCN-01 treatments induced only a low percentage of sub-G_1 cells (Fig. 5B). Nevertheless, apoptotic cell death was increased in the presence of 100 μmol/L of monastrol (from 9% to 22%). Similar conclusions were obtained by measuring cell death by Trypan blue exclusion assays (Fig. 5C).

Collectively, these results indicate that a relatively low concentration of monastrol, itself not causing significant cell death, can promote the cell death induced with IR and UCN-01.

Monastrol and checkpoint abrogation reduce long-term cell survival

We next examined the effects of checkpoint abrogation and monastrol on long-term survival of cancer cells by clonogenic survival assays. Results using IR alone indicated that approximately 75% and 50% survival after cells were irradiated with approximately 1 and 2 Gy of IR, respectively (Fig. 6A). Likewise, titration with different concentrations of monastrol alone indicated that more than 80% clonogenic survival after cells were treated with 100 μmol/L of monastrol (Fig. 6B). Cells were next treated with different doses of IR, together with UCN-01 and monastrol (100 μmol/L). After 12 hours incubation, the UCN-01 and monastrol were washed away; and the cells were incubated further for clonogenic survival assays. Figure 6C shows that although treatment with IR and UCN-01 caused some degree of cell growth inhibition, addition of monastrol reduced the clonogenic survival further. Collectively, our data indicate that cell proliferation could be effectively attenuated using a DNA damage and checkpoint abrogation strategy in conjunction with the inhibition of Eg5 with monastrol.

Discussion

In this study, we tested the idea of whether the combination of the G_2 DNA damage checkpoint, checkpoint abrogation, and Eg5 inhibition could enhance the population of cells undergoing mitotic catastrophe. The central idea is that cells exhibit different fates after checkpoint abrogation. They either undergo apoptosis during mitosis or progress into the following interphase. It is likely that the survived cells are more prone to further genome instability and may develop into more aggressive tumors. Therefore from the view point of cancer therapies, it is desirable to eliminate as many cancer cells as possible during the first mitosis.

For HeLa cells treated with IR followed by UCN-01, more than 90% of the cells were forced into mitosis prematurely (Figs. 2C and 3E). While approximately 40% cells underwent mitotic catastrophe, the rest of the cells were able to survive and enter G_1 phase. We found that mitotic catastrophe was enhanced after Eg5 was inactivated, either with siRNAs (Fig. 2) or monastrol (Figs. 3E and 4). This was confirmed by assays including measurement of PARP cleavage (Figs. 2B and 4A), sub-G_1 cells (Figs. 2A and 4B), and live cell imaging (Figs. 2C and 3E).

In agreement with the increase in checkpoint abrogation–mediated mitotic catastrophe by Eg5 inhibition, we found

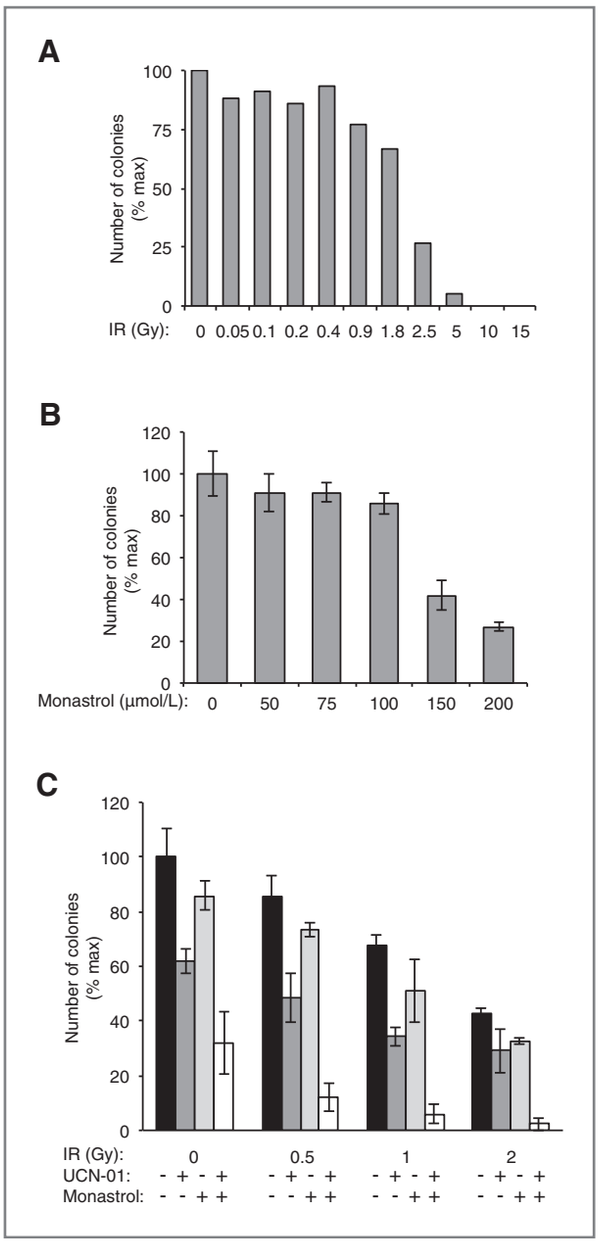

Figure 6. Monastrol and checkpoint abrogation reduce long-term cell survival. A, dose-dependent inhibition of clonogenic survival by IR. HeLa cells were irradiated with different doses of IR as indicated. After 2 weeks, the colonies were fixed and visualized by staining with crystal violet. The number of colonies was quantified. B, concentration-dependent inhibition of clonogenic survival by monastrol. HeLa cells were treated with different concentrations of monastrol. After 16 hours of incubation, the cells were washed and reseeded. After 2 weeks, the colonies were fixed, visualized by staining with crystal violet, and quantified. Mean ± SD of 3 independent experiments are shown. C, monastrol further reduces the clonogenic survival caused by checkpoint abrogation. HeLa cells were mock-irradiated or irradiated with 0.5, 1, or 2 Gy of IR. The cells were treated with UCN-01 in the absence or presence of monastrol as indicated. After 16 hours of incubation, the cells were washed and reseeded. After 2 weeks, the colonies were fixed, visualized by staining with crystal violet, and quantified. Mean ± SD of 3 independent experiments are shown.

that monastrol reduced the clonogenic survival after IR and UCN-01 treatment (Fig. 6C). A caveat is that UCN-01 alone also reduced cell survival. This DNA damage-independent cell death was presumably due to the functions of CHK1 in normal DNA replicative folk progression. The cell death induced by UCN-01 alone cannot be simply additive with other treatments when used in combination. This is because in our study, UCN-01 was applied to IR-treated cells only after they have already passed S-phase and arrested in G_2 phase. This again highlights the importance of the order of the treatments: checkpoint bypass and Eg5 inhibition should be applied only after the DNA damage checkpoint is activated.

Corroboration with checkpoint abrogation probably did not require the complete inactivation of Eg5 functions, as residual Eg5 was presumably still present after siRNA-mediated depletion (Fig. 2B). Furthermore, a relatively low concentration of monastrol (100 μmol/L) was sufficient to promote mitotic catastrophe (Fig. 3E). Although treatment with this concentration of monastrol alone increased the duration of mitosis [as indicated by both histone $H3^{Ser10}$ phosphorylation (Fig. 3A) and direct measurement of mitotic time (Fig. 3C)], it neither blocked cells in mitosis nor induced cell death [as indicated by flow cytometry (Fig. 3B) and live cell imaging (Fig. 3E and Supplementary Fig. S1)]. We believe that the extension of mitosis caused by Eg5 siRNA or 100 μmol/L of monastrol was sufficient in promoting mitotic catastrophe. This is in agreement with the conclusion of our previous studies, in which mitotic catastrophe was increased when mitosis was extended by depletion of $p31^{comet}$ or CDC20 (4). Interestingly, not all the drugs that delayed mitosis we tested were able to increase cell death associated with IR and UCN-01 treatments. For example, inhibitors of PLK1 or Aurora A were less effective in this regard (our unpublished data). The underlying reasons and which other types of drugs are effective in promoting mitotic catastrophe awaits further investigation.

Other factors that govern the extent of mitotic catastrophe after checkpoint abrogation are the dose of IR and the nature of the cell line (4). IR treatment followed by checkpoint abrogation in other cell lines, including H1299, HCT116, U2OS, induced significantly less mitotic catastrophe than HeLa cells (4). However, we found that monastrol was also able to sensitize H1299 cells after checkpoint abrogation (Fig. 5B and C). Hence, it is likely that the combined treatment with monastrol can be beneficial for treating cancer cells that exhibit resistance to IR and UCN-01. For future clinical use, the order of the treatments is likely to be of crucial importance. Our studies indicated that the Eg5 inhibitor and checkpoint abrogator should be introduced only after the DNA damage checkpoint is activated.

The clinical use of monastrol is limited by the high dosages needed to achieve complete Eg5 inhibition (18). Moreover, such high dosages of monastrol are associated with a variety of side effects, including neurotoxicity. Sensory neurons appear to be particularly sensitive to prolonged exposure of monastrol (18). Monastrol was also shown to affect growth of dendrites and axons in primary cortical neuron cultures (19). By combining checkpoint abrogation and Eg5 inhibition, a relatively low concentration of monastrol was already highly effective in enhancing mitotic catastrophe. This should reduce mitotic arrest and subsequent apoptosis for normal mitotic cells and minimize the neurotoxicity. Moreover, the principle of the current study should be applicable to other newer generation of Eg5 inhibitors at various stages of development and clinical trials (20). Whether newer generation of Eg5 inhibitors can promote mitotic catastrophe more effectively than monastrol should warrant further cell line and animal studies.

In conclusion, we found that although not all cancer cells were eliminated by mitotic catastrophe after checkpoint abrogation, cell death could be enhanced by inhibition of Eg5 with either siRNAs or monastrol. A relatively low concentration of monastrol, alone not sufficient in causing mitotic arrest, was effective in promoting mitotic catastrophe when combined with checkpoint abrogation.

Disclosure of Potential Conflicts of Interest

No potential conflicts of interest were disclosed.

Acknowledgments

The authors thank members of the Poon laboratory for constructive criticism on the manuscript.

Grant Support

This work was supported in part by the Research Grants Council grants 662208 and AOE-MG/M-08/06 to R.Y.C. Poon.

The costs of publication of this article were defrayed in part by the payment of page charges. This article must therefore be hereby marked *advertisement* in accordance with 18 U.S.C. Section 1734 solely to indicate this fact.

Received October 12, 2011; revised January 23, 2012; accepted March 14, 2012; published OnlineFirst April 20, 2012.

References

1. Ma HT, Poon RYC. How protein kinases co-ordinate mitosis in animal cells. Biochem J 2011;435:17–31.
2. Smith J, Tho LM, Xu N, Gillespie DA. The ATM-Chk2 and ATR-Chk1 pathways in DNA damage signaling and cancer. Adv Cancer Res 2010;108:73–112.
3. Vitale I, Galluzzi L, Castedo M, Kroemer G. Mitotic catastrophe: a mechanism for avoiding genomic instability. Nat Rev Mol Cell Biol 2011;12:385–92.
4. On KF, Chen Y, Ma HT, Chow JP, Poon RYC. Determinants of mitotic catastrophe on abrogation of the G2 DNA damage checkpoint by UCN-01. Mol Cancer Ther 2011;10:784–94.
5. Lawrence CJ, Dawe RK, Christie KR, Cleveland DW, Dawson SC, Endow SA, et al. A standardized kinesin nomenclature. J Cell Biol 2004;167:19–22.
6. Cochran JC, Sontag CA, Maliga Z, Kapoor TM, Correia JJ, Gilbert SP. Mechanistic analysis of the mitotic kinesin Eg5. J Biol Chem 2004;279:38861–70.
7. Ding S, Xing N, Lu J, Zhang H, Nishizawa K, Liu S, et al. Overexpression of Eg5 predicts unfavorable prognosis in non-

muscle invasive bladder urothelial carcinoma. Int J Urol 2011;18: 432–8.
8. Liu M, Wang X, Yang Y, Li D, Ren H, Zhu Q, et al. Ectopic expression of the microtubule-dependent motor protein Eg5 promotes pancreatic tumourigenesis. J Pathol 2010;221:221–8.
9. Castillo A, Morse HCr, Godfrey VL, Naeem R, Justice MJ. Overexpression of Eg5 causes genomic instability and tumor formation in mice. Cancer Res 2007;67:10138–47.
10. Mayer TU, Kapoor TM, Haggarty SJ, King RW, Schreiber SL, Mitchison TJ. Small molecule inhibitor of mitotic spindle bipolarity identified in a phenotype-based screen. Science 1999;286:971–4.
11. Huszar D, Theoclitou ME, Skolnik J, Herbst R. Kinesin motor proteins as targets for cancer therapy. Cancer Metastasis Rev 2009;28:197–208.
12. Yam CH, Siu WY, Lau A, Poon RYC. Degradation of cyclin A does not require its phosphorylation by CDC2 and cyclin-dependent kinase 2. J Biol Chem 2000;275:3158–67.
13. Chan YW, Ma HT, Wong W, Ho CC, On KF, Poon RYC. CDK1 inhibitors antagonize the immediate apoptosis triggered by spindle disruption but promote apoptosis following the subsequent rereplication and abnormal mitosis. Cell Cycle 2008;7:1449–61.
14. Siu WY, Arooz T, Poon RYC. Differential responses of proliferating versus quiescent cells to adriamycin. Exp Cell Res 1999;250:131–41.
15. Chan YW, On KF, Chan WM, Wong W, Siu HO, Hau PM, et al. The kinetics of p53 activation versus cyclin E accumulation underlies the relationship between the spindle-assembly checkpoint and the postmitotic checkpoint. J Biol Chem 2008;283: 15716–23.
16. Yam CH, Siu WY, Kaganovich D, Ruderman JV, Poon RYC. Cleavage of cyclin A at R70/R71 by the bacterial protease OmpT. Proc Natl Acad Sci U S A 2001;98:497–501.
17. Poon RYC, Toyoshima H, Hunter T. Redistribution of the CDK inhibitor p27 between different cyclin.CDK complexes in the mouse fibroblast cell cycle and in cells arrested with lovastatin or ultraviolet irradiation. Mol Biol Cell 1995;6:1197–213.
18. Haque SA, Hasaka TP, Brooks AD, Lobanov PV, Baas PW. Monastrol, a prototype anti-cancer drug that inhibits a mitotic kinesin, induces rapid bursts of axonal outgrowth from cultured postmitotic neurons. Cell Motil Cytoskeleton 2004;58:10–6.
19. Yoon SY, Choi JE, Huh JW, Hwang O, Lee HS, Hong HN, et al. Monastrol, a selective inhibitor of the mitotic kinesin Eg5, induces a distinctive growth profile of dendrites and axons in primary cortical neuron cultures. Cell Motil Cytoskeleton 2005;60:181–90.
20. Knight SD, Parrish CA. Recent progress in the identification and clinical evaluation of inhibitors of the mitotic kinesin KSP. Curr Top Med Chem 2008;8:888–904.